Electronic Supplementary Information for

Oxidized Magnetic Au Single Atom on Doped TiO_2(110) Becomes a High Performance CO Oxidation Catalyst due to Charge Effect

Jinlei Shi[ab], Xingju Zhao[a], Liying Zhang[a], Xinlian Xue[a], Z. X. Guo[c],Y.F. Gao[d,e], S. F. Li[a*]

[a]*International Laboratory for Quantum Functional Materials of Henan, School of Physics and Engineering, Zhengzhou University, Zhengzhou, Henan 450001, China*

[b]*Beijing Computational Science Research Center, Beijing 100193, P.R. China*

[c]*Department of Chemistry, University College London, London WC1H 0AJ, UK*

[d]*Department of Materials Science and Engineering, University of Tennessee, Knoxville, Tennessee 37996, USA*

[e]*Materials Science and Technology Division, Oak Ridge National Laboratory, Oak Ridge, Tennessee 37831, USA*

This file includes:

S1: Atomic structure and coordinates of the rutile c(4×2) TiO_2(110) substrate with a surface oxygen vacancy.
S2: Optimized structures for single Au atom deposited on the rutile TiO_2(110) surface.
S3: Optimized structure for O_2 adsorption on the Au@TiO_2(110) SAC.
S4: Optimized structure for the nickel-doped Au@TiO_2(110) complex, i.e., Au@(Ni) TiO_2(110).
S5: Optimized geometric configuration of the O_2 molecule adsorption on the Ni doped Au@TiO_2(110) system and the associated orbital analysis.
S6: Electronic charge density analysis for CO and O_2 co-adsorption on Au@(Ni)TiO_2(110).
S7: The optimized configuration of O_2 adsorption on the bow-shaped O-Au-O complex resulted by the first round of CO oxidation.
S8: Optimized structures and formation energies for the TM doped Au@TiO_2(110) complexes (TM = *Co, Pt, Ru, Rh, Cu, Ni and Al*).

S1: Atomic structure and coordinates of the rutile c(4×2) TiO_2(110) substrate with a surface oxygen vacancy.

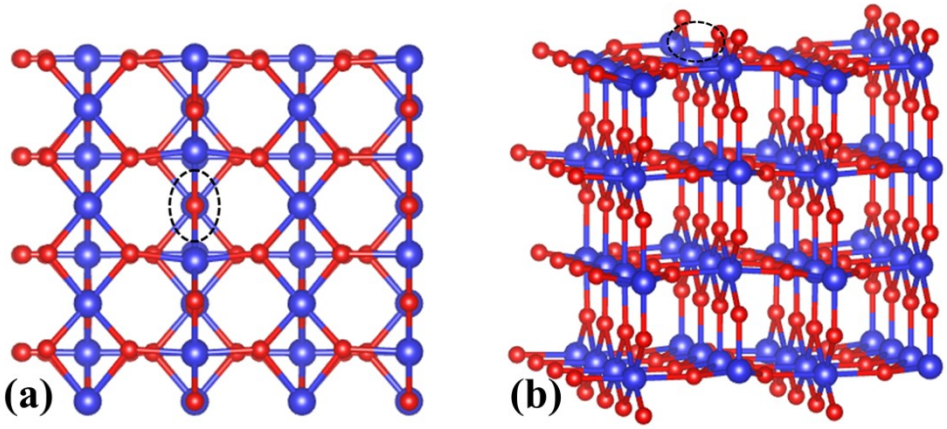

Fig. S1 *(Color online) Optimized structure of rutile TiO_2(110) substrate with surface oxygen vacancy (V_O) site:* ***(a)*** *top view and* ***(b)*** *side view. Black circle represents the surface oxygen vacancy site.*

Atomic coordinates of the rutile c(4×2) TiO_2(110) substrate with a surface oxygen vacancy.

Ti(0.0499999999999972 0.300075393328236 0.500313640753116)	Ti(0.549999999999997 0.799014049767597 0.497934310450931)
Ti(0.0499999999999972 0.0499999999999972 0.378076067325345)	Ti(0.549999999999997 0.549999999999997 0.375587236899508)
Ti(0.0499999999999972 0.299973619298072 0.229295604857007)	Ti(0.549999999999997 0.800040621565941 0.229279406550539)
Ti(0.0499999999999972 0.0499999999999972 0.106019133869573)	Ti(0.549999999999997 0.549999999999997 0.105120668111737)
Ti(0.176832645717552 0.0499999999999972 0.514741285936405)	Ti(0.690928674583581 0.549999999999997 0.502289236136926)
Ti(0.173802626741406 0.298968552869278 0.366355858750542)	Ti(0.675799396076101 0.801016945241858 0.365655677918294)
Ti(0.175046532268098 0.0499999999999972 0.239667382562338)	Ti(0.674734959592932 0.549999999999997 0.238347048473698)
Ti(0.175004140418764 0.29981840149901 0.0920071621495353)	Ti(0.675105795153186 0.800356574097378 0.0919368230949615)
Ti(0.299234749456784 0.300583352644466 0.499018899648367)	Ti(0.800765250543217 0.799416647355521 0.499018899648367)
Ti(0.300132212244904 0.0499999999999972 0.377495432292532)	Ti(0.80130911076916 0.549999999999997 0.37133760619615)
Ti(0.299953683909869 0.300174452091873 0.229010580270426)	Ti(0.800046316090124 0.79982554790812 0.229010580270426)
Ti(0.299952071522028 0.0499999999999972 0.106481963765702)	Ti(0.800110128867942 0.549999999999997 0.10607251392976)
Ti(0.425591777992237 0.0499999999999972 0.514053235170797)	Ti(0.927706902990084 0.549999999999997 0.516851073693337)
Ti(0.424200603923893 0.298983054758136 0.365655677918294)	Ti(0.926197373258587 0.801031447130715 0.366355858750542)
Ti(0.424815519305703 0.0499999999999972 0.239319524887164)	Ti(0.925894479565066 0.549999999999997 0.238749182806735)
Ti(0.424894204846808 0.299643425902615 0.0919368230949615)	Ti(0.92499585958123 0.800181598500984 0.0920071621495353)
Ti(0.549999999999997 0.300985950232397 0.497934310450931)	Ti(0.172293097009909 0.549999999999997 0.516851073693337)
Ti(0.549999999999997 0.0499999999999972 0.377022891462953)	Ti(0.173802626741406 0.801031447130715 0.366355858750542)
Ti(0.549999999999997 0.299959378434046 0.229279406550539)	Ti(0.17410552043492 0.549999999999997 0.238749182806735)
Ti(0.549999999999997 0.0499999999999972 0.10595036284787)	Ti(0.175004140418764 0.800181598500984 0.0920071621495353)
Ti(0.674408222007757 0.0499999999999972 0.514053235170797)	Ti(0.299234749456784 0.799416647355521 0.499018899648367)
Ti(0.675799396076101 0.298983054758136 0.365655677918294)	Ti(0.298690889230833 0.549999999999997 0.37133760619615)

Ti(0.675184480694291 0.0499999999999972 0.239319524887164)	Ti(0.299953683909869 0.79982554790812 0.229010580270426)
Ti(0.675105795153186 0.299643425902615 0.0919368230949615)	Ti(0.299889871132052 0.549999999999997 0.10607251392976)
Ti(0.800765250543217 0.300583352644466 0.499018899648367)	Ti(0.409071325416413 0.549999999999997 0.502289236136926)
Ti(0.79986778775509 0.0499999999999972 0.377495432292532)	Ti(0.424200603923893 0.801016945241858 0.365655677918294)
Ti(0.800046316090124 0.300174452091873 0.229010580270426)	Ti(0.425265040407062 0.549999999999997 0.238347048473698)
Ti(0.800047928477965 0.0499999999999972 0.106481963765702)	Ti(0.424894204846808 0.800356574097378 0.0919368230949615)
Ti(0.923167354282441 0.0499999999999972 0.514741285936405)	Ti(0.0499999999999972 0.799924606671764 0.500313640753116)
Ti(0.926197373258587 0.298968552869278 0.366355858750542)	Ti(0.0499999999999972 0.549999999999997 0.378511491350923)
Ti(0.924953467731896 0.0499999999999972 0.239667382562338)	Ti(0.0499999999999972 0.800026380701922 0.229295604857007)
Ti(0.92499585958123 0.29981840149901 0.0920071621495353)	Ti(0.0499999999999972 0.549999999999997 0.105319840860566)
O(0.7922768420049 0.549999999999997 0.558211430676611)	O(0.549999999999997 0.300740098841648 0.421150478364604)
O(0.799816330630811 0.79887277339832 0.421307710315328)	O(0.549999999999997 0.0499999999999972 0.289347004938001)
O(0.799598777078294 0.549999999999997 0.289288329324726)	O(0.549999999999997 0.29872092646547 0.150893844760673)
O(0.79997958068948 0.797155459763978 0.150466633498602)	O(0.549999999999997 0.30002417963086 0.0457958004746573)
O(0.80003254722331 0.802346963330663 0.0457460107265248)	O(0.549999999999997 0.0499999999999972 0.454321847873845)
O(0.80739220572972 0.549999999999997 0.452804856770438)	O(0.549999999999997 0.301418574734565 0.31585705387421)
O(0.799914932109429 0.799017656021751 0.315703346491026)	O(0.549999999999997 0.0499999999999972 0.182922289674763)
O(0.800006224389321 0.549999999999997 0.183558250221494)	O(0.671267691378493 0.398759568186263 0.511804359975298)
O(0.915970944543196 0.895392618306549 0.511898524863653)	O(0.674778704177371 0.148565889810708 0.370879145970545)
O(0.925164878814521 0.647496694747649 0.370773212118928)	O(0.67512948029573 0.399289909273932 0.234006676451429)
O(0.924330071724803 0.898500502763141 0.233594787632867)	O(0.675519858523912 0.14351289222931 0.0935544391914149)
O(0.924864047991228 0.643359154570831 0.0931113332850657)	O(0.673045981705569 0.208437201287625 0.511416657950314)
O(0.917624287393639 0.703043740847676 0.513846598300439)	O(0.67510897035262 0.452748203911629 0.371854166852532)
O(0.924610298798937 0.951833036059937 0.371598117575683)	O(0.67510076799023 0.201728372144423 0.233685052630953)
O(0.924616069376377 0.70078194835947 0.23396422225538)	O(0.675524685449509 0.456628562322258 0.0929631518479397)
O(0.924514029594284 0.956446487591065 0.0935777603568795)	O(0.797087271524397 0.0499999999999972 0.560396204810016)
O(0.0499999999999972 0.0499999999999972 0.559714356133121)	O(0.799816330630811 0.301127226601674 0.421307710315328)
O(0.0499999999999972 0.301678441066969 0.419744324978366)	O(0.799632181658893 0.0499999999999972 0.289489678612405)
O(0.0499999999999972 0.0499999999999972 0.289721561285226)	O(0.79997958068948 0.302844540236016 0.150466633498602)
O(0.0499999999999972 0.300504353652719 0.151048069837678)	O(0.80003254722331 0.297653036669331 0.0457460107265248)
O(0.0499999999999972 0.299998753057479 0.0458106023067444)	O(0.798045255500066 0.0499999999999972 0.454599121487098)
O(0.0499999999999972 0.0499999999999972 0.455069573291679)	O(0.799914932109429 0.300982343978243 0.315703346491026)
O(0.0499999999999972 0.299420211117261 0.315112514156524)	O(0.80001130048754 0.0499999999999972 0.183754165701046)
O(0.0499999999999972 0.0499999999999972 0.182990124539628)	O(0.917624287393639 0.396956259152317 0.513846598300439)
O(0.182375712606354 0.396956259152317 0.513846598300439)	O(0.924610298798937 0.148166963940057 0.371598117575683)
O(0.175389701201056 0.148166963940057 0.371598117575683)	O(0.924616069376377 0.399218051640524 0.23396422225538)
O(0.175383930623624 0.399218051640524 0.23396422225538)	O(0.924514029594284 0.143553512408928 0.0935777603568795)
O(0.175485970405709 0.143553512408928 0.0935777603568795)	O(0.915970944543196 0.204607381693444 0.511898524863653)
O(0.184029055456798 0.204607381693444 0.511898524863653)	O(0.925164878814521 0.452503305252352 0.370773212118928)
O(0.174835121185472 0.452503305252352 0.370773212118928)	O(0.924330071724803 0.201499497236852 0.233594787632867)
O(0.175669928275191 0.201499497236852 0.233594787632867)	O(0.924864047991228 0.456640845429163 0.0931113332850657)
O(0.175135952008766 0.456640845429163 0.0931113332850657)	O(0.0499999999999972 0.549999999999997 0.563915463211244)
O(0.302912728475596 0.0499999999999972 0.560396204810016)	O(0.0499999999999972 0.798321558933024 0.419744324978366)

O(0.300183669369183 0.301127226601674 0.421307710315328)	O(0.0499999999999972 0.549999999999997 0.289307051439358)
O(0.300367818341101 0.0499999999999972 0.289489678612405)	O(0.0499999999999972 0.799495646347274 0.151048069837678)
O(0.300020419310513 0.302844540236016 0.150466633498602)	O(0.0499999999999972 0.800001246942514 0.0458106023067444)
O(0.299967452776684 0.297653036669331 0.0457460107265248)	O(0.0499999999999972 0.549999999999997 0.457441466940804)
O(0.301954744499928 0.0499999999999972 0.454599121487098)	O(0.0499999999999972 0.800579788882733 0.315112514156524)
O(0.300085067890564 0.300982343978243 0.315703346491026)	O(0.0499999999999972 0.549999999999997 0.182827702089632)
O(0.299988699512454 0.0499999999999972 0.183754165701046)	O(0.184029055456798 0.895392618306549 0.511898524863653)
O(0.428732308621501 0.398759568186263 0.511804359975298)	O(0.174835121185472 0.647496694747649 0.370773212118928)
O(0.425221295822622 0.148565889810708 0.370879145970545)	O(0.175669928275191 0.898500502763141 0.233594787632867)
O(0.424870519704263 0.399289909273932 0.234006676451429)	O(0.175135952008766 0.643359154570831 0.0931113332850657)
O(0.424480141476081 0.14351289222931 0.0935544391914149)	O(0.182375712606354 0.703043740847676 0.513846598300439)
O(0.426954018294425 0.208437201287625 0.511416657950314)	O(0.175389701201056 0.951833036059937 0.371598117575683)
O(0.424891029647374 0.452748203911629 0.371854166852532)	O(0.175383930623624 0.70078194835947 0.23396422225538)
O(0.424899232009764 0.201728372144423 0.233685052630953)	O(0.175485970405709 0.956446487591065 0.0935777603568795)
O(0.424475314550484 0.456628562322258 0.0929631518479397)	O(0.307723157995093 0.549999999999997 0.558211430676611)
O(0.549999999999997 0.0499999999999972 0.559923775098419)	O(0.300183669369183 0.79887277339832 0.421307710315328)
O(0.299967452776684 0.802346963330663 0.0457460107265248)	O(0.300401222921699 0.549999999999997 0.289288329324726)
O(0.29260779427028 0.549999999999997 0.452804856770438)	O(0.300020419310513 0.797155459763978 0.150466633498602)
O(0.300085067890564 0.799017656021751 0.315703346491026)	O(0.549999999999997 0.549999999999997 0.289327969182586)
O(0.299993775610673 0.549999999999997 0.183558250221494)	O(0.549999999999997 0.801279073534523 0.150893844760673)
O(0.426954018294425 0.891562798712375 0.511416657950314)	O(0.549999999999997 0.799975820369134 0.0457958004746573)
O(0.424891029647374 0.647251796088365 0.371854166852532)	O(0.549999999999997 0.549999999999997 0.457642071232978)
O(0.424899232009764 0.898271627855571 0.233685052630953)	O(0.549999999999997 0.798581425265428 0.31585705387421)
O(0.424475314550484 0.643371437677736 0.0929631518479397)	O(0.549999999999997 0.549999999999997 0.182769084836614)
O(0.428732308621501 0.701240431813731 0.511804359975298)	O(0.673045981705569 0.891562798712375 0.511416657950314)
O(0.425221295822622 0.951434110189286 0.370879145970545)	O(0.67510897035262 0.647251796088365 0.371854166852532)
O(0.424870519704263 0.700710090726062 0.234006676451429)	O(0.67510076799023 0.898271627855571 0.233685052630953)
O(0.424480141476081 0.956487107770684 0.0935544391914149)	O(0.675524685449509 0.643371437677736 0.0929631518479397)
O(0.549999999999997 0.799259901158345 0.421150478364604)	O(0.671267691378493 0.701240431813731 0.511804359975298)
O(0.67512948029573 0.700710090726062 0.234006676451429)	O(0.674778704177371 0.951434110189286 0.370879145970545)
O(0.675519858523912 0.956487107770684 0.0935544391914149)	

S2: Optimized structures for single Au atom deposited on the rutile TiO_2(110) surface.

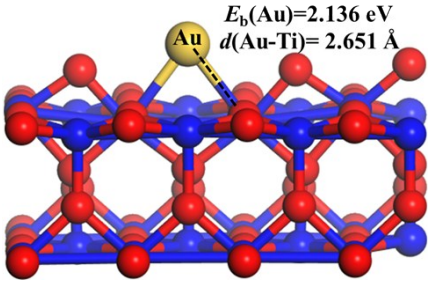

Fig. S2 *(Color online) Optimized structure of a Au monomer adsorption on the surface oxygen vacancy (V_O) site of rutile TiO_2(110) substrate which is denoted as Au@TiO_2(110). Red, blue, and yellow spheres represent the O, Ti, and Au atoms, respectively.*

As shown in **Fig. S2**, the optimized Au single atom prefers to locate at the surface oxygen vacancy (V_O) site on TiO_2(110) surface. Note that if we manually put the Au atom slightly away from the V_O site, the Au monomer will automatically relax back to the V_O site, which is in accordance with the experimental observation that surface V_O sites play a dominant role in stabilizing gold monomers.[1] The binding energy of the Au monomer is: E_b(Au)=2.136 eV. Here, the E_b(Au) is defined as: $E_b(Au)=-(E(Au@TiO_2(110))-E(Au_{atom})-E(TiO_2(110)))$, wherein the terms of $E(Au_{atom})$, $E(TiO_2(110))$, and $E(Au@TiO_2(110))$ represent the total energy of the isolated gas phase Au atom, the total energy of defective TiO_2(110) substrate, and that of the Au@TiO_2(110) complex, respectively. The average bond length between the Au and nearby Ti atoms d(Au-Ti) is 2.651 Å.

S3: Optimized structure for O_2 adsorption on the Au@TiO_2(110) SAC.

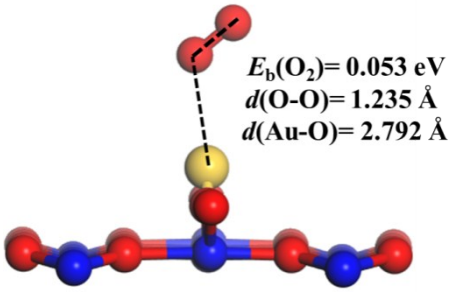

Fig. S3 *(Color online) Local configuration of the optimized structure for O_2 adsorption on the Au@TiO_2(110) complex. Red, blue, and yellow spheres represent the O, Ti, and Au atoms, respectively.*

As shown in **Fig. S3**, our calculated results show that the O_2 molecule can only very weakly adsorb on the supported Au monomer with a d(Au-O)=2.792 Å and an exothermic adsorption energy of 0.053 eV. Note that the bond length of the adsorbed O_2 molecule keeps almost intact as compared to that in its gas phase, 1.24 Å, indicating that the Au SAC is highly inert to active O_2. For clarity purpose, here we

only show the top-most surface atoms of the TiO_2(110) substrate.

S4: Optimized structure for nickel-doped the Au@TiO_2(110) complex, i.e., Au@(Ni) TiO_2(110).

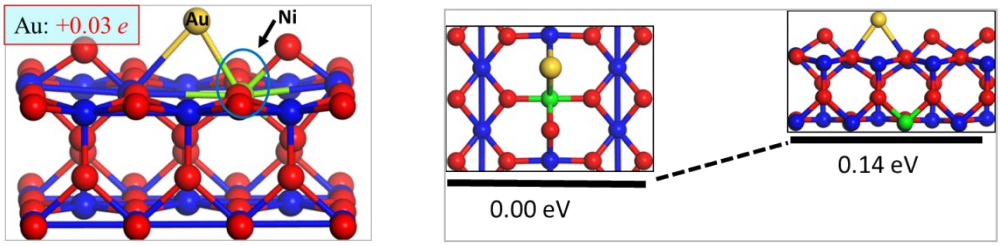

Fig. S4 *(Color online) Local configuration of the optimized geometric structure of nickel-doped Au@TiO_2(110) complex.*

As illustrated in **Fig. S4**, it is found that the Ni dopant favors to substitute the Ti atom nearby the V_O site. Note that our calculations show that if the Ni atom is located in other site away from the present location, the total energy significantly increases. For example, when the Ni atom is located at the subsurface Ti site, it is about 0.14 eV higher in energy. In the preferred Ni-doped Au@TiO_2(110) complex shown in **Fig. S4**, the Au monomer is slightly oxidized and positively charged by about 0.03 e, which is confirmed by Bader charge analysis.

Here, we also calculated the formation energies (E_f) of the Ni dopants, which is defined as

$$E_f = E(Au@(Ni)TiO_2(110)) - E(Au@TiO_2(110)) + \mu(Ti) - \mu(Ni)$$

Where $E(Au@(Ni)TiO_2(110))$, $E(Au@TiO_2(110))$, $\mu(Ti)$, and $\mu(Ni)$ are the total energies of Ni substitutional doped Au@TiO_2(110), pristine Au@TiO_2(110), chemical potential of Ti, and Ni atom, respectively. The calculated E_f is 1.96 eV.

S5: Optimized geometric configuration of the O_2 molecule adsorption on the Ni doped Au@TiO_2(110) system and the associated orbital analysis.

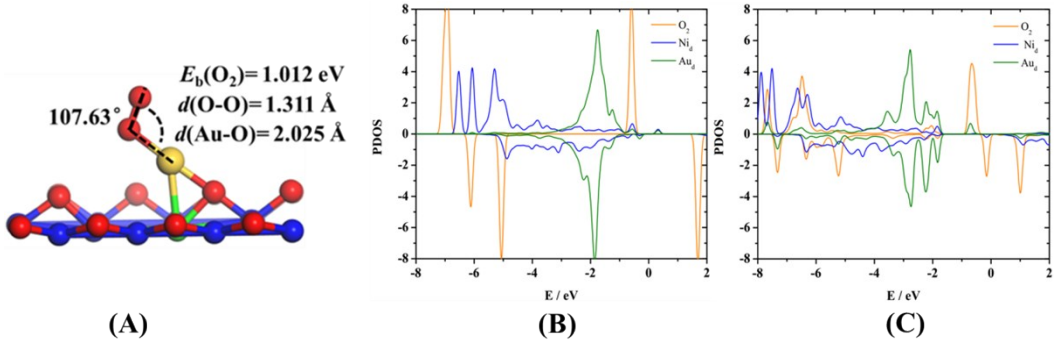

Fig. S5 *(Color online) Local configuration of the optimized geometric structure of O_2 adsorption on Ni-doped Au@TiO_2(110) complex,* ***(A)****; the initial stages of an O_2 molecule approaching toward (B) Au,* ***(B)*** *and upon O_2 adsorption,* ***(C)****.*

Based on our extensive calculations, we identify the most stable adsorption configuration of the O_2 molecule on the slightly oxidized Au monomer in the Ni-doped Au@TiO_2(110) complex, as shown in **Fig. S5(A)**. Specifically, the O_2 molecule prefers an end-on structure, forming an angle ∠O-O-Au=107.63°. In addition, the binding of the O_2 molecule with the Au SAC is mainly accompanied with the hybridization of the oxygen 2pπ* orbital with the HOMO of Au. Particularly, part of the antibonding 2pπ* electronic state of O_2 are now shifted downward below the E_F, see **Fig. S5(B)**, confirming the occurrence of charge transfer from the Au SAC to the O_2 molecule, which results in an enlarged O-O bond length (1.31 Å) and leads to an exothermic adsorption energy of 1.012 eV. Furthermore, the stretching vibrational frequency of the adsorbed O_2 species has been red-shifted to 1158.87 cm^{-1} from the calculated value of 1560.83 cm^{-1} for the case of gas phase.

S6: Electronic charge density analysis for CO and O_2 co-adsorption on Au@(Ni)TiO_2(110).

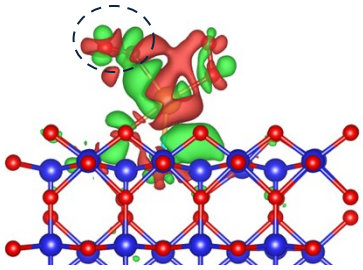

Fig. S6 *(Color online) Electronic charge density analysis for CO and O_2 co-adsorption on Au@(Ni)TiO_2(110). Here, charge difference is presented: Δρ=ρ(CO-O_2-Au@(Ni)TiO_2(110))-ρ(CO)-ρ(O_2-Au@(Ni)TiO_2(110)).*

we have performed additional electronic analysis for CO co-adsorption and provided the charge difference, Δρ, which is defined as: Δρ=ρ(CO-O_2-Au@(Ni)TiO_2(110))-ρ(CO)-ρ(O_2-Au@(Ni)TiO_2(110)). In the above formula, the first, second and the third terms correspond to the optimized electronic charges of the CO and O_2 co-adsorbed structure on Ni-doped Au@TiO_2(110), i.e., CO-O_2-Au@(Ni)TiO_2(110), the adsorbed CO species, and the O_2-Au@(Ni)TiO_2(110) component, respectively. Note that for the latter two terms, the CO and O_2-Au@(Ni)TiO_2(110) maintain exactly the same configuration as that in the first term, i.e., CO-O_2-Au@(Ni)TiO_2(110). In **Fig. S6**, we present such a Δρ with the isosurface of *0.005 e/Å^3*.

One can see that, from **Fig. S6**, the classic back-donation interaction mechanism is well exhibited for CO adsorption: CO donates 5σ electrons to the Au@(Ni)TiO_2(110) substrate and back-donates from the Au@(Ni)TiO_2(110) substrate into the unoccupied π* orbital of the CO species, as confirmed by the electron depletion (in red) and electron accumulation (in green) highlighted by the dashed circle, respectively.

S7: The optimized configuration of O_2 adsorption on the bow-shaped O-Au-O complex resulted by the first round of CO oxidation.

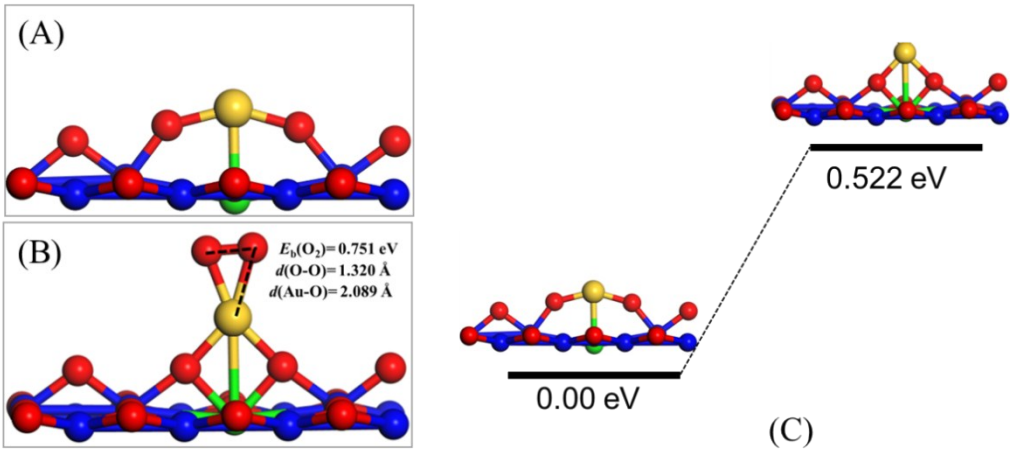

Fig. S7 *(Color online) Optimized geometric configurations of the O-Au-O SAC generated by finishing the first round of CO oxidation, as shown in Fig. 2 of the main text,* ***(A)****;* O_2 *adsorption on the structure shown in* ***Fig. S7(A)***, ***(B)****. The energetic diagram of structure* ***(A)*** *and the one generated by removing the adsorbed* O_2 *species,* ***(C)****.*

In **Fig. S7(A),** we show the optimized geometric structure of the O-Au-O SAC complex obtained by releasing the CO_2 molecule in the first round of CO oxidation shown in Fig. 2 of the main text. Upon the reaction of CO_{ad}+O-O_{ad}→CO_2+ O_{ad}, when the first CO molecule is oxidized and the generated CO_2 molecule is released, there is still one O atom left from the dissociated O_2 molecule, which prefers to readily heal the oxygen vacancy site of Au@TiO_2(110) complex. After such a healing process, a novel bow-shaped O-Au-O structure is formed, as shown in **Fig. S7(A).** Notably, the Au monomer forms strong chemical bonds with two neighboring O atoms, with an exothermic energy of 3.101 eV and a bond length *d*(Au-Ni) of 2.568 Å, respectively. Furthermore, we confirmed that the Au atom is now highly oxidized (probably due to the larger electronegativity of the Ni atom), i.e., Q(Au)=+0.64 *e*, which is obtained by Bader charge analysis.

Note that in the present bow-shaped O-Au-O structure, the O_2 molecule can be significantly activated on the Au monomer, with an exothermic energy of 0.751 eV. Specifically, in contrast to the above cases wherein the O_2 molecule only bind with the Au atom with one O atom directly contacting with the Au atom, now both O atoms bind with the Au monomer, and the O-O bond length of the adsorbed O_2 species has been enlarged to 1.320 Å, and the average bond length of the two Au-O bonds is 2.089 Å, respectively, see structure shown in **Fig. S7(B).**

Note that as shown in **Fig. S7(B), a** relatively smaller binding energy of the O_2 molecule on the Au monomer in the bow-shaped O-Au-O complex is obtained, as

compared to that when the O_2 molecule is adsorbed on the structure shown in **Fig. S5(A)**. However, we claim that in **Fig. S7(B)**, the O_2 molecule is more strongly activated, as reflected by the enlarged O-O bond length (1.320 Å) and further red-shifted O-O vibrational frequency ($\nu(O_2)$=1128.6 cm^{-1}), as compared to that (1158.9 cm^{-1}) shown in **Fig. S5(A)**. Additional calculations show that it is due to the energy cost compensating (**Fig. S7(C)**) the local structural O-Au-Ni-O reconstruction upon O_2 adsorption as shown in **Fig. S7(B)**.

S8: Optimized structures and formation energies for the TM doped Au@TiO_2(110) complexes (TM = *Co, Pt, Ru, Rh, Cu, Ni and Al*).

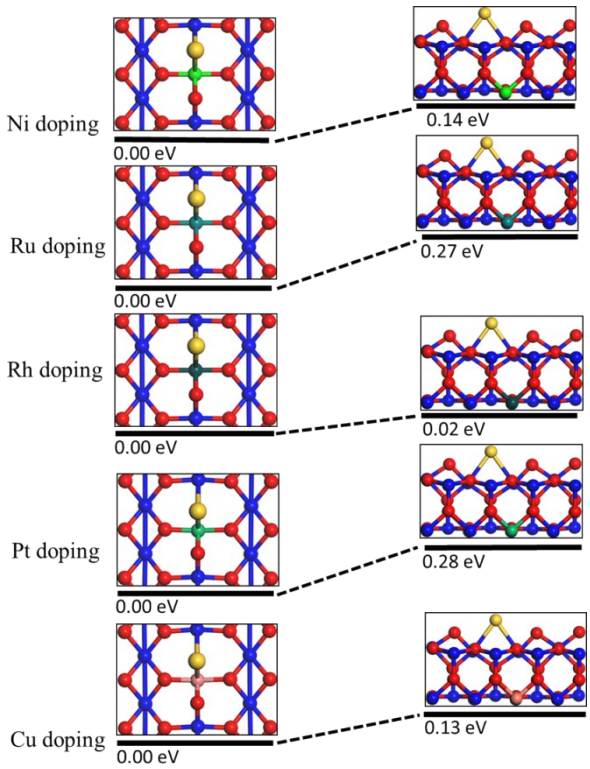

Fig. S8 *(Color online) Optimized geometric structures of TM atom doped Au@TiO_2(110) complexes (TM = Ni, Ru, Rh, Pt, Cu). In the structures presented in the left column, the dopant metal atoms are located in the first layer, and in the right column, the dopants are in the subsurface layer.*

Here, four additional transition mental (TM) elements (Ru, Rh, Pt, and Cu) with different values of the electronegativity are considered as the dopants. As shown in **Fig. S8**, the structures are similar to the Ni doped structure presented in **Fig. S4**, and all these elements are identified to prefer the same site to stabilize the Au atom.

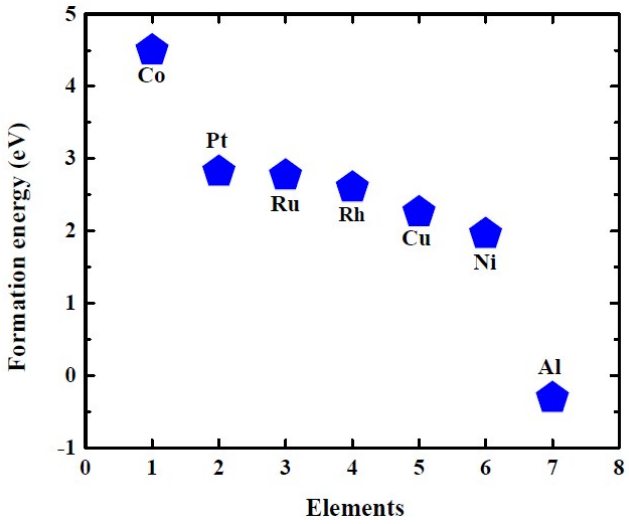

Fig. S9 Formation energy of TM and metal atoms (TM=Co, Pt, Ru, Rh, Cu, Ni and Al) in TiO_2(110).

Furthermore, we also calculated the formation energies (E_f) of the above dopants, which is defined as

$$E_f = E(Au@(TM)TiO_2(110)) - E(Au@TiO_2(110)) + \mu(Ti) - \mu(TM)$$

Where $E(Au@(TM)TiO_2(110))$, $E(Au@TiO_2(110))$, $\mu(Ti)$, and $\mu(TM)$ are the total energies of TM substitutional doped $Au@TiO_2(110)$, pristine $Au@TiO_2(110)$, chemical potential of Ti, and TM atoms, respectively. As shown in **Fig. S9**, the calculated values of the E_f are 4.50, 2.82, 2.77, 2.60, 2.26, 1.96 and -0.31 eV for Co, Pt, Ru, Rh, Cu, Ni, and Al respectively. Significantly, the E_f of Pt, Ru, Rh, Cu, and Ni are lying between that of Co and Al which have been demonstrated to be readily doped in both anatase and rutile TiO_2.

1. Matthey, D.; Wang, J. G.; Wendt, S.; Matthiesen, J.; Schaub, R.; Lægsgaard, E.; Hammer, B.; Besenbacher, F. Enhanced Bonding of Gold Nanoparticles on Oxidized TiO_2(110). *Science* **2007,** *315* (5819), 1692-1696.